

7 Supplementary material for LHCb-PAPER-2015-042

Figures 4 and 5 are simply colour versions of the B&W figures used in the main body, suitable for slides. Fig. 7 collects a set of plots of the $\ln \chi_{\text{IP}}^2$ projection of the second fit in slices of decay time.

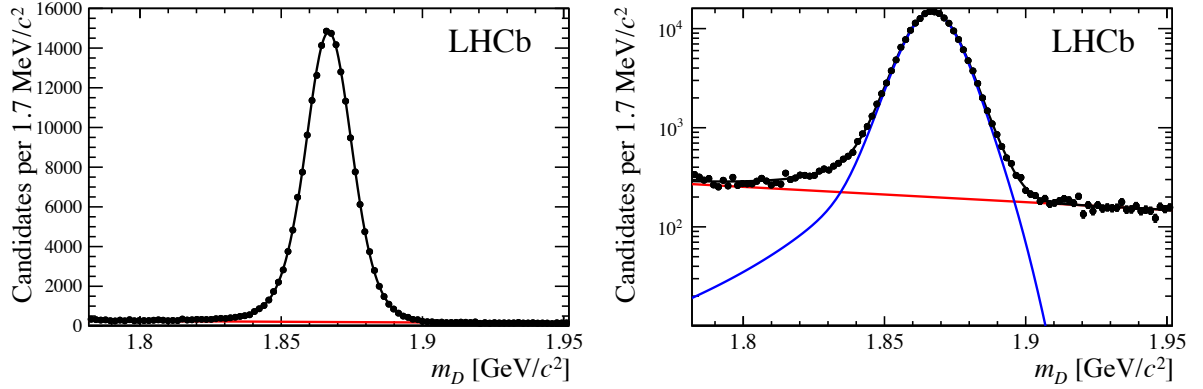


Figure 4: Colour version of Fig. 1. Fitted m_D distribution. Both plots show the same data sample with linear (left) and logarithmic (right) vertical scales. The curves show the results of the first fit, described in Sec. 4.2: the total (solid black), the background component (red), and the signal component (blue, right only).

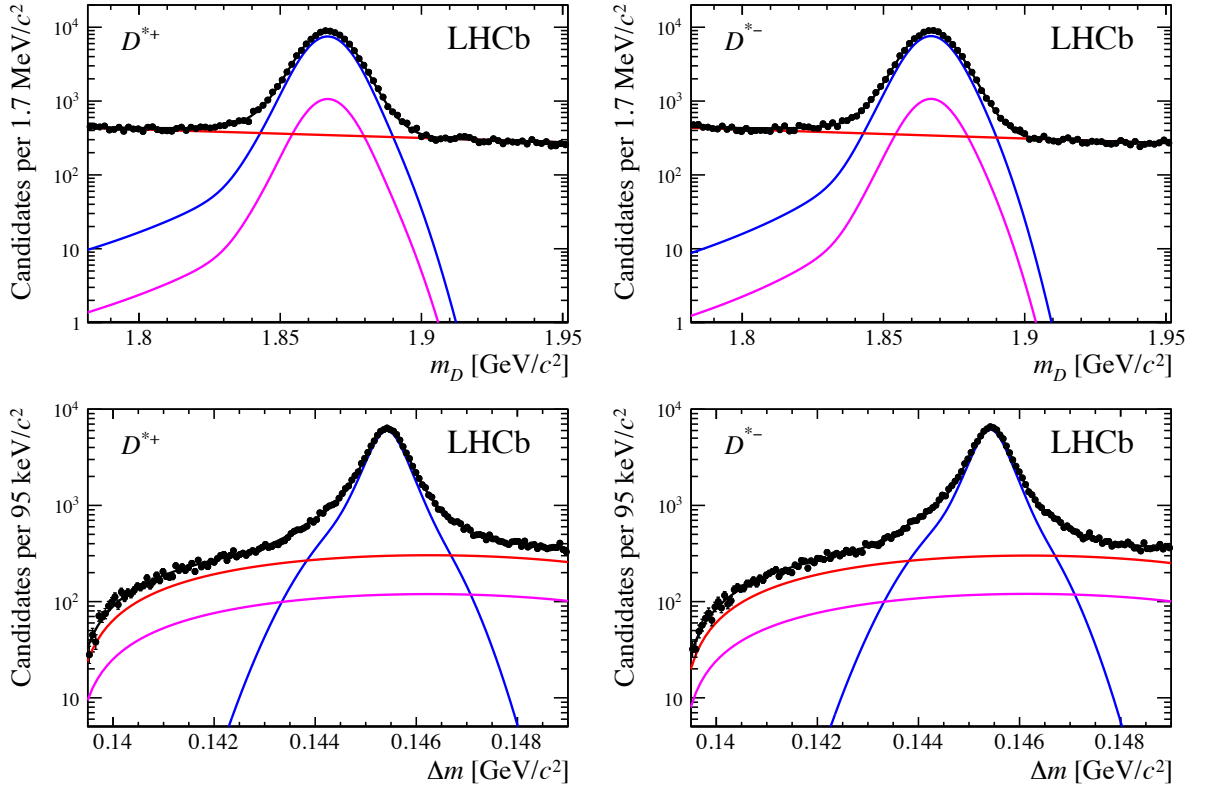


Figure 5: Colour version of Fig. 3. Fitted $(m_D, \Delta m)$ distributions. The upper row shows the m_D projection and the lower row Δm . The left column shows D^{*+} candidates and the right column D^{*-} . The signal and background components are shown separately (signal in blue, D^0 background magenta, combinatoric background red, and the sum as solid black).

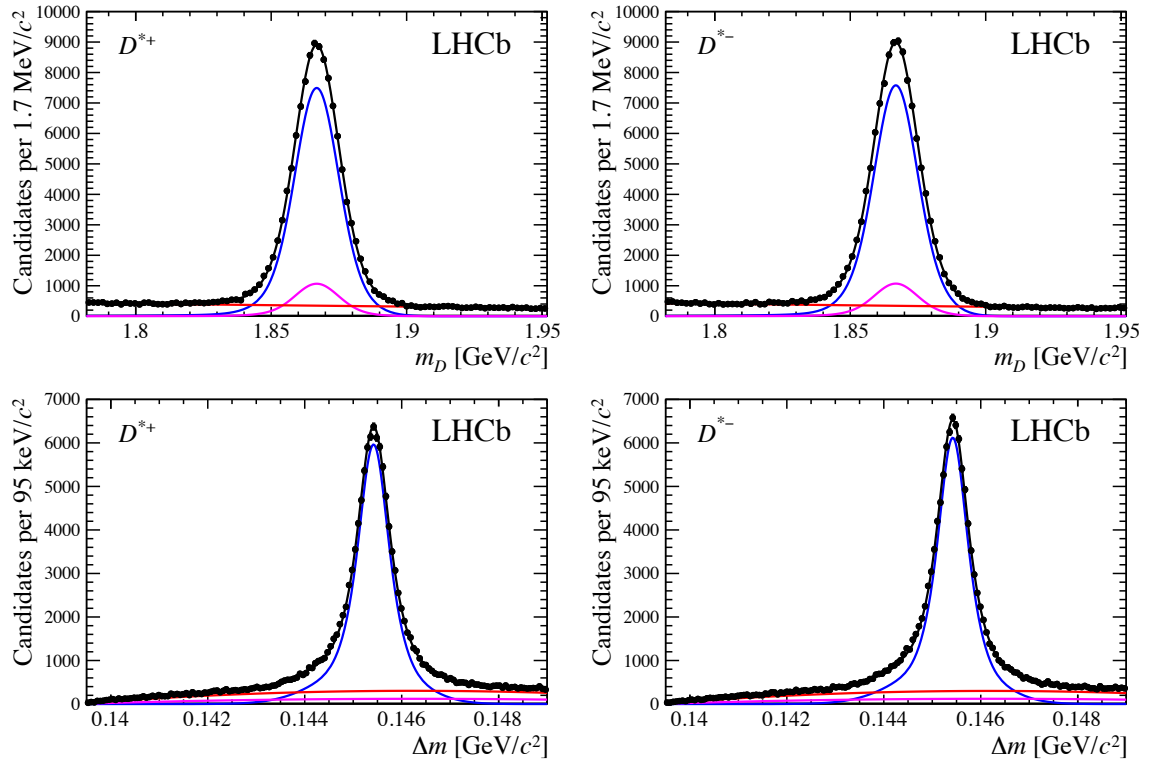


Figure 6: [Linear-scale version of Fig. 3](#). Fitted $(m_D, \Delta m)$ distributions. The upper row shows the m_D projection and the lower row Δm . The left column shows D^{*+} candidates and the right column D^{*-} . The signal and background components are shown separately (signal in blue, D^0 background magenta, combinatoric background red, and the sum as solid black).

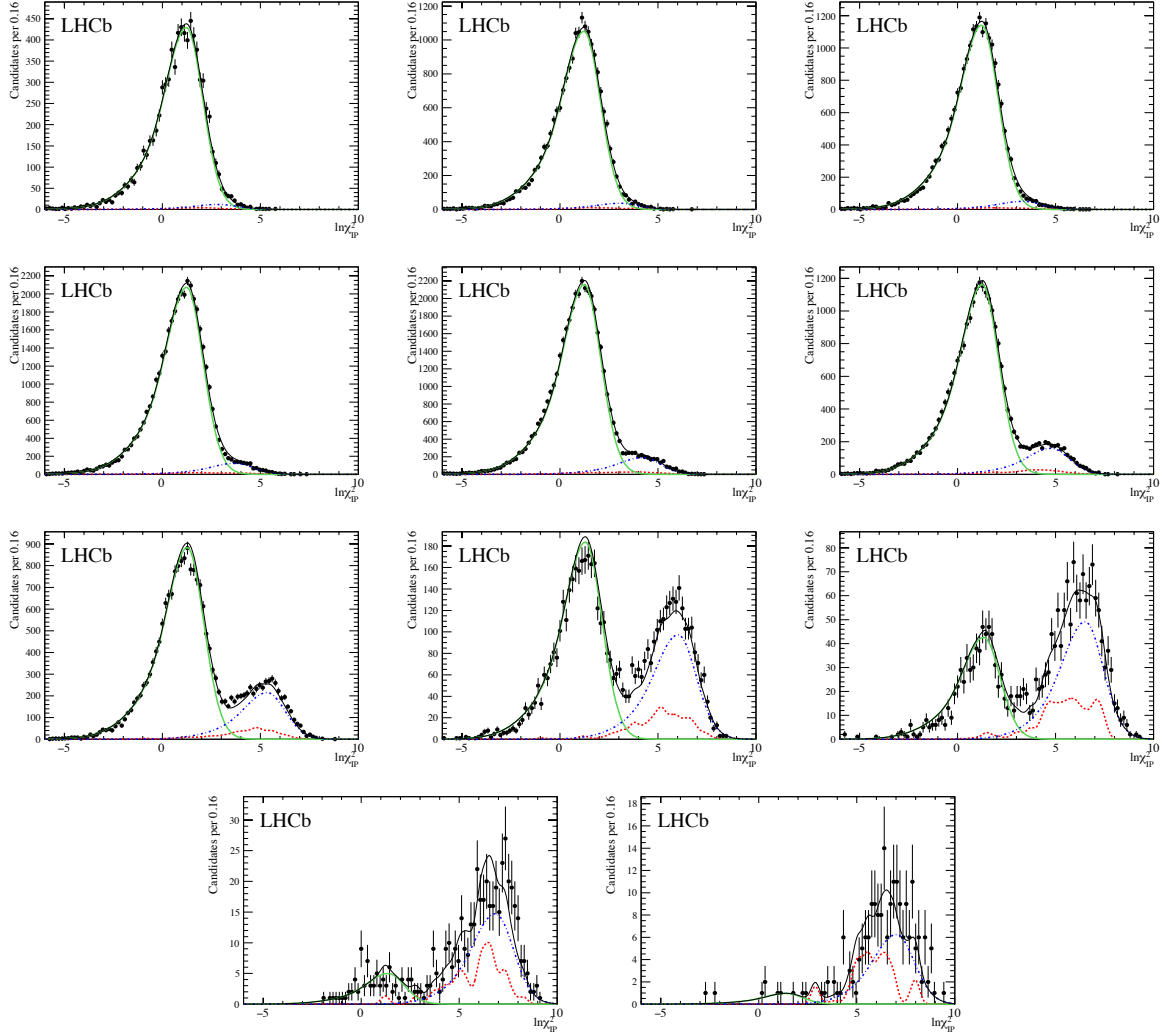


Figure 7: **Additional plots.** The $\ln \chi_{\text{IP}}^2$ projection from the fit for separation of prompt and secondary candidates. The curves show the results of the second fit, described in Sec. 4.4, in slices of decay time. The components are: the total (solid black), the prompt component (solid green) the secondary component (dot-dashed blue), and the combinatorial component (dashed red). From top left to bottom right, the slices of t_D are: 0.30–0.35, 0.35–0.45, 0.45–0.55, 0.55–0.75, 0.75–1.05, 1.05–1.35, 1.35–2.00, 2.00–2.65, 2.65–3.55, 3.55–4.25, 4.25–5.00 ps. In the final bins ($t_D > 2.65$ ps), the number of events in the mass sidebands is small and fluctuations are visible in the nonparametric combinatorial background PDF.

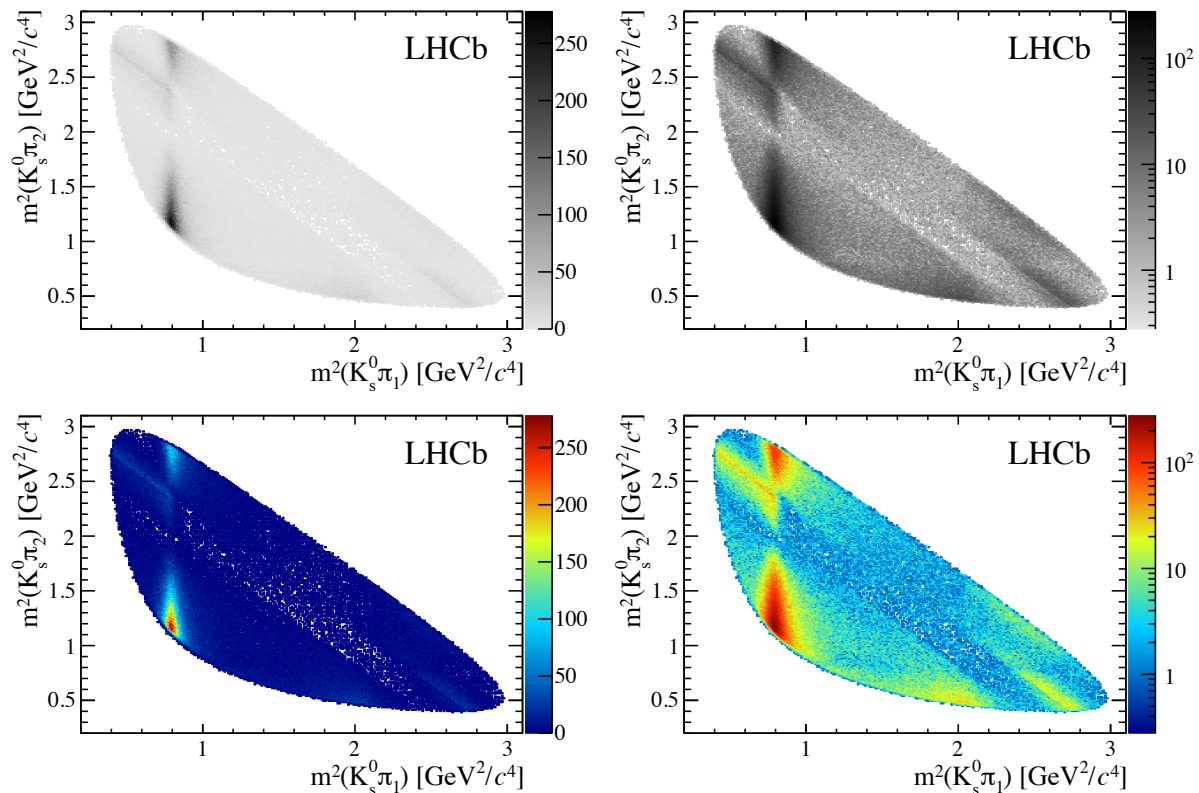


Figure 8: **Additional plots.** The Dalitz plot distribution of candidates in data passing the full selection (see Sec. 3) and inside the narrow 2D ($m_D, \Delta m$) signal window (defined in Sec. 4.1). Both $D^{*+} \rightarrow D^0 \pi^+$ and $D^{*-} \rightarrow \bar{D}^0 \pi^-$ candidates are included. The x -axis is $m^2(K_s^0 \pi_1)$ and the y -axis is $m^2(K_s^0 \pi_2)$, where π_1 has opposite charge to the soft pion, and π_2 has the same charge. (One can tell which is which by the strong CF $D^0 \rightarrow K^*(892)^- \pi^+$ contribution.) All four plots have the exact same content, but with different colour schemes and with log or linear intensity scales. Because the K_s^0 mass is not constrained to the nominal value in the reconstruction, the Dalitz plot boundary is smeared and there is a border region with fewer events per bin.